Research Report

96-53

Modeling and Control of Multi-Phase Induction Machine with Structural Unbalance, Part 2: Field Oriented Control and Experimental Verification

Y. Zhao*, T.A. Lipo

*GE Corporate R&D Center
1 River Road
Schenectady, NY 12301

Wisconsin Power Electronics Research Center
University of Wisconsin-Madison
Madison WI 53706-1691

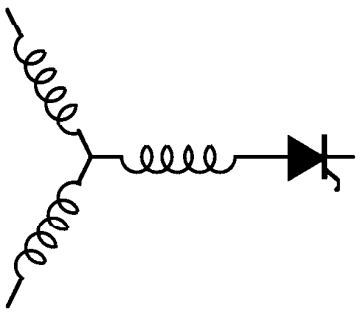

Wisconsin
Electric
Machines &
Power
Electronics
Consortium

University of Wisconsin-Madison
College of Engineering
Wisconsin Power Electronics Research Center
2559D Engineering Hall
1415 Engineering Drive
Madison WI 53706-1691

MODELING AND CONTROL OF A MULTI-PHASE INDUCTION MACHINE WITH STRUCTURAL UNBALANCE

Part II. Field-Oriented Control and Experimental Verification

Yifan Zhao
GE Corporate R&D Center
1 River Road
Schenectady, NY 12301

Thomas A. Lipo
University of Wisconsin-Madison
1415 Johnson Drive
Madison, WI 53706

***Abstract*: Field-oriented control techniques for a multi-phase induction machine with an unbalanced stator winding structure is presented in this paper. An unbalanced stationary to synchronous reference frame transformation for stator current was developed in this paper to deal with the asymmetrical structure and thus make the field-oriented control techniques developed from balanced machine winding structure become applicable. Experimental tests were conducted on a dual three phase induction machine with a open phase to verify the proposed analytical modeling and control techniques.**

***Key words*: Multi-phase induction machine, unbalanced operation, field-oriented control.**

I. INTRODUCTION

Using the concept of vector space decomposition, the electromechanical energy conversion property of the induction machine investigated in this paper has been previously represented by a d-q plane machine model [1]. This model is an equivalent two phase induction machine with asymmetrical stator windings of different number of turns. Because of the asymmetrical structure, field oriented-control techniques developed from machines with balanced winding structure can not be employed directly. To achieve field-oriented control, an unbalanced stationary to synchronous reference frame transformation for stator current was developed. With this transformation applied to the machine, a symmetrical two phase induction machine model was obtained, thus making existing field-oriented control techniques to become applicable.

To verify the proposed analytical modeling and control technique, a dual three phase induction machine (with one phase open) drive system has been built and tested. The experimental results have demonstrated very good agreement with the theoretical analysis.

96 WM 149-5 EC A paper recommended and approved by by the IEEE Electric Machinery Committee of the IEEE Power Engineering Society for presentation at the 1996 IEEE/PES Winter Meeting, January 21-25, 1996, Baltimore, MD. Manuscript submitted August1, 1995; made available for printing January 2, 1996.

II. FIELD-ORIENTED CONTROL WITH STRUCTURAL UNBALANCE

A. Field-Oriented Machine Equations

The stationary reference frame d-q plane equation of the machine investigated in this paper can be expressed as [1]:

$$\begin{bmatrix} v^s_{ds} \\ v^s_{qs} \end{bmatrix} = \begin{bmatrix} r_s & 0 \\ 0 & r_s \end{bmatrix} \cdot \begin{bmatrix} i^s_{ds} \\ i^s_{qs} \end{bmatrix} + \frac{d}{dt} \begin{bmatrix} \lambda^s_{ds} \\ \lambda^s_{qs} \end{bmatrix} \tag{1}$$

$$\begin{bmatrix} 0 \\ 0 \end{bmatrix} = \begin{bmatrix} r_r & 0 \\ 0 & r_r \end{bmatrix} \cdot \begin{bmatrix} i^s_{dr} \\ i^s_{qr} \end{bmatrix} + \frac{d}{dt} \begin{bmatrix} \lambda^s_{dr} \\ \lambda^s_{qr} \end{bmatrix} + \begin{bmatrix} 0 & -\omega_r \\ \omega_r & 0 \end{bmatrix} \cdot \begin{bmatrix} \lambda^s_{dr} \\ \lambda^s_{qr} \end{bmatrix} \tag{2}$$

$$T_e = \frac{P}{2} \frac{1}{L_r} (M_q i^s_{qs} \lambda^s_{dr} - M_d i^s_{ds} \lambda^s_{qr}) \tag{3}$$

where:

$$\begin{bmatrix} \lambda^s_{ds} \\ \lambda^s_{qs} \end{bmatrix} = \begin{bmatrix} L_{ds} & 0 \\ 0 & L_{qs} \end{bmatrix} \cdot \begin{bmatrix} i^s_{ds} \\ i^s_{qs} \end{bmatrix} + \begin{bmatrix} M_d & 0 \\ 0 & M_q \end{bmatrix} \cdot \begin{bmatrix} i^s_{dr} \\ i^s_{qr} \end{bmatrix} \tag{4}$$

$$\begin{bmatrix} \lambda^s_{dr} \\ \lambda^s_{qr} \end{bmatrix} = \begin{bmatrix} M_d & 0 \\ 0 & M_q \end{bmatrix} \cdot \begin{bmatrix} i^s_{ds} \\ i^s_{qs} \end{bmatrix} + \begin{bmatrix} L_r & 0 \\ 0 & L_r \end{bmatrix} \cdot \begin{bmatrix} i^s_{dr} \\ i^s_{qr} \end{bmatrix} \tag{5}$$

Eqs. (1) through (5) suggest that, after one of the six phases of the dual three phase induction machine is open-circuited, the machine is equivalent, from the point of view of electromechanical energy conversion, to a two phase machine with asymmetrical d-q windings as shown in Fig. 1.

Typical field-oriented control of induction machine is accomplished by locking a synchronous reference frame to rotor flux linkage vector. The rotation transformation of machine variables from a stationary reference frame to the synchronous reference frame for balanced operation is [4]:

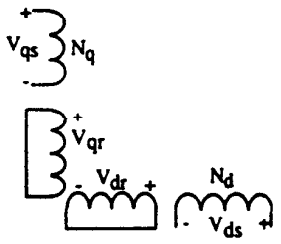

Fig. 1 Asymmetrical Stator Winding Two Phase Machine

$$[T(\theta_e)]=\begin{bmatrix}\cos(\theta_e) & \sin(\theta_e)\\ -\sin(\theta_e) & \cos(\theta_e)\end{bmatrix} \tag{6}$$

where θ_e is the angle between the two reference frames.

For the unbalanced operating situation investigated in this paper, the rotation transformation is still applicable to the rotor variables since the rotor maintains a balanced structure. However, to overcome the effect of an asymmetrical stator winding structure and thereby to obtain smooth output torque, unbalanced excitation must be provided to the machine. As a consequence, the transformation of stator variables using the balanced transformation (6) would result in ac components in the synchronous reference frame, that are certainly not desirable for the purpose of field-oriented control. In this regard, it is necessary to redefine the rotation transformation for stator variables.

Since the rotor has a balanced structure and thus balanced flux linkage, to produce smooth torque, the stator MMF must be balanced as well [5]. Therefore, the rotation transformation (6) is applicable to the stator MMF. That is:

$$\begin{bmatrix}f^e_{ds}\\ f^e_{qs}\end{bmatrix}=\begin{bmatrix}\cos(\theta_e) & \sin(\theta_e)\\ -\sin(\theta_e) & \cos(\theta_e)\end{bmatrix}\cdot\begin{bmatrix}f^s_{ds}\\ f^s_{qs}\end{bmatrix} \tag{7}$$

where f is used to represent MMF.

Assuming the number of turns of the stator windings in the equivalent machine model in Fig. 1 are N_d and N_q respectively, the stator MMF can be expressed as:

$$\begin{bmatrix}f^s_{ds}\\ f^s_{qs}\end{bmatrix}=\begin{bmatrix}N_d & 0\\ 0 & N_q\end{bmatrix}\cdot\begin{bmatrix}i^s_{ds}\\ i^s_{qs}\end{bmatrix} \tag{8}$$

Substituting (8) into (7) and reorganizing the result we have:

$$\begin{bmatrix}f^e_{ds}\\ f^e_{qs}\end{bmatrix}=\sqrt{N_dN_q}\begin{bmatrix}\sqrt{\frac{N_d}{N_q}}\cos(\theta_e) & \sqrt{\frac{N_q}{N_d}}\sin(\theta_e)\\ -\sqrt{\frac{N_d}{N_q}}\sin(\theta_e) & \sqrt{\frac{N_q}{N_d}}\cos(\theta_e)\end{bmatrix}\cdot\begin{bmatrix}i^s_{ds}\\ i^s_{qs}\end{bmatrix} \tag{9}$$

Assuming the pole arcs under the two stator windings are equal, then:

$$\frac{N_d}{N_q}=\frac{M_d}{M_q} \tag{10}$$

and

$$\begin{bmatrix}f^e_{ds}\\ f^e_{qs}\end{bmatrix}=\sqrt{N_dN_q}\begin{bmatrix}\sqrt{\frac{M_d}{M_q}}\cos(\theta_e) & \sqrt{\frac{M_q}{M_d}}\sin(\theta_e)\\ -\sqrt{\frac{M_d}{M_q}}\sin(\theta_e) & \sqrt{\frac{M_q}{M_d}}\cos(\theta_e)\end{bmatrix}\cdot\begin{bmatrix}i^s_{ds}\\ i^s_{qs}\end{bmatrix} \tag{11}$$

or

$$\begin{bmatrix}\frac{f^e_{ds}}{\sqrt{N_dN_q}}\\ \frac{f^e_{ds}}{\sqrt{N_dN_q}}\end{bmatrix}=\begin{bmatrix}\sqrt{\frac{M_d}{M_q}}\cos(\theta_e) & \sqrt{\frac{M_q}{M_d}}\sin(\theta_e)\\ -\sqrt{\frac{M_d}{M_q}}\sin(\theta_e) & \sqrt{\frac{M_q}{M_d}}\cos(\theta_e)\end{bmatrix}\cdot\begin{bmatrix}i^s_{ds}\\ i^s_{qs}\end{bmatrix} \tag{12}$$

Defining:

$$\begin{bmatrix}\frac{f^e_{ds}}{\sqrt{N_dN_q}}\\ \frac{f^e_{ds}}{\sqrt{N_dN_q}}\end{bmatrix}=\begin{bmatrix}i^e_{ds}\\ i^e_{qs}\end{bmatrix} \tag{13}$$

we finally have:

$$\begin{bmatrix}i^e_{ds}\\ i^e_{qs}\end{bmatrix}=\begin{bmatrix}\sqrt{\frac{M_d}{M_q}}\cos(\theta_e) & \sqrt{\frac{M_q}{M_d}}\sin(\theta_e)\\ -\sqrt{\frac{M_d}{M_q}}\sin(\theta_e) & \sqrt{\frac{M_q}{M_d}}\cos(\theta_e)\end{bmatrix}\cdot\begin{bmatrix}i^s_{ds}\\ i^s_{qs}\end{bmatrix} \tag{14}$$

Eq. (14) is the stator current rotation transformation we have been looking for. With this transformation, the stator windings in the synchronous reference frame will be made equivalent to a pair of balanced d-q windings as depicted in Fig. 2. It should be pointed out that although the windings and the stator currents in the synchronous reference frame are somewhat fictitious, their physical meaning in terms of torque production is quite clear. That is, they produce the same magnetic field as the original stator windings and thus induce the same rotor dynamic response and produce the same electromagnetic torque.

In (2), applying the normal rotation transformation (6) to rotor variables and the transformation (14) to stator currents, the following synchronous reference frame equation results:

$$\begin{bmatrix}0\\ 0\end{bmatrix}=\begin{bmatrix}r_r & 0\\ 0 & r_r\end{bmatrix}\cdot\begin{bmatrix}i^e_{dr}\\ i^e_{qr}\end{bmatrix}+\frac{d}{dt}\begin{bmatrix}\lambda^e_{dr}\\ \lambda^e_{qr}\end{bmatrix}+\begin{bmatrix}0 & -(\omega_e-\omega_r)\\ (\omega_e-\omega_r) & 0\end{bmatrix}\cdot\begin{bmatrix}\lambda^e_{dr}\\ \lambda^e_{qr}\end{bmatrix} \tag{15}$$

The rotor flux linkage vector in (5) is transformed to the synchronous reference frame as:

$$\begin{bmatrix}\lambda^e_{dr}\\ \lambda^e_{qr}\end{bmatrix}=\begin{bmatrix}\sqrt{M_dM_q} & 0\\ 0 & \sqrt{M_dM_q}\end{bmatrix}\cdot\begin{bmatrix}i^e_{ds}\\ i^e_{qs}\end{bmatrix}+\begin{bmatrix}L_r & 0\\ 0 & L_r\end{bmatrix}\cdot\begin{bmatrix}i^e_{dr}\\ i^e_{qr}\end{bmatrix} \tag{16}$$

The electromagnetic torque of the machine expressed in the synchronous frame is:

$$T_e=\frac{P}{2}\frac{\sqrt{M_dM_q}}{L_r}(i^e_{qs}\lambda^e_{dr}-i^e_{ds}\lambda^e_{qr}) \tag{17}$$

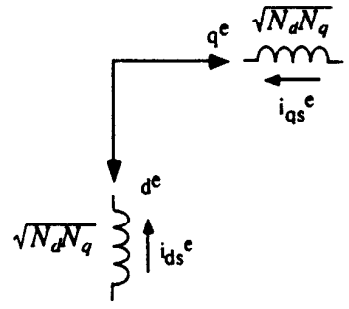

Fig. 2 Synchronous Frame d q Machine Model

The dynamics of the stator in the synchronous reference frame has been ignored due to an assumption that the machine is fed by a current regulated inverter.

With the choice of rotor flux vector as the synchronous reference frame and aligning it to the d^e-axis, (15) through (17) can be further reduced to:

$$0 = r_r i^e_{dr} + \frac{d}{dt}\lambda^e_{dr} \tag{18}$$

$$0 = r_r i^e_{qr} + (\omega_e - \omega_r)\lambda^e_{dr} \tag{19}$$

$$\lambda^e_{dr} = \sqrt{M_d M_q}\, i^e_{ds} + L_r i^e_{dr} \tag{20}$$

$$\lambda^e_{qr} = \sqrt{M_d M_q}\, i^e_{qs} + L_r i^e_{qr} = 0 \tag{21}$$

$$T_e = \frac{P}{2}\frac{\sqrt{M_d M_q}}{L_r} i^e_{qs}\lambda^e_{dr} \tag{22}$$

The slip relation and the relation between the rotor flux linkage and the magnetizing component of stator current can be derived form above equations as:

$$\omega_e - \omega_r = s\omega_e = \frac{r_r}{L_r}\frac{\sqrt{M_d M_q}\, i^e_{qs}}{\lambda^e_{dr}} \tag{23}$$

$$(L_r p + r_r)\cdot\lambda^e_{dr} = r_r \cdot \sqrt{M_d M_q}\cdot i^e_{ds} \tag{24}$$

A block diagram of the machine under rotor flux oriented control is sketched in Fig. 3.

It can be observed that (18) through (22) are identical in form to the rotor flux-oriented dynamic equations of an induction machine with balanced winding structure [4]. The only difference is in the value of the air gap magnetizing inductance. One should not be surprised concerning this result since the equivalent machine that is now being dealt with is indeed a balanced winding machine (see Fig. 2) after one applies the unbalanced rotation transformation to the unbalanced stator excitation. The stator windings of this machine are the geometric mean of the windings of the asymmetrical d-q machine model in Fig. 1. In other words,

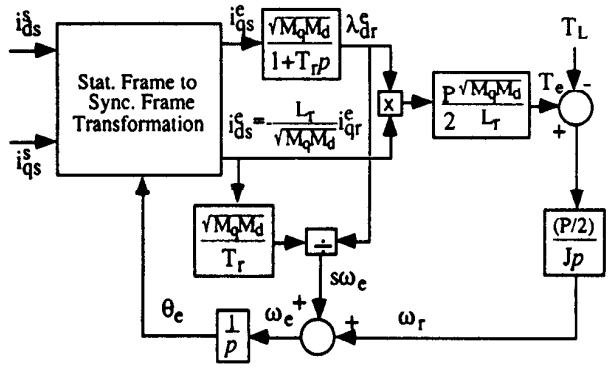

Fig. 3 Block Diagram of Rotor Flux Oriented Machine

the air gap magnetizing inductance of the equivalent machine is $\sqrt{M_d M_q}$, here M_d and M_q are the d-axis and the q-axis air gap magnetizing inductances of the asymmetrical machine respectively.

B. Field-Oriented Control Scheme

Since the rotor flux-oriented equations of an asymmetrical winding induction machine have the same form as a symmetrical winding machine, all the rotor flux-oriented control techniques are still applicable. There are two basic means to achieve rotor flux field orientation: indirect and direct. Indirect field-oriented control can be realized by controlling the slip frequency to satisfy (23). Direct field-orientation, which relies directly upon the knowledge of the rotor flux linkage vector and thus being physically insightful, will be adopted for the purpose of testing the theoretical results.

The implementation of a direct field-oriented controller requires that the position and the amplitude of the rotor flux linkage vector to be known. Usually, this is accomplished by the employment of a rotor flux estimator. The implementation of the rotor flux linkage estimator used in this paper is illustrated as follows.

The d-q subspace rotor voltage equation and flux in the rotor reference frame can be expressed as:

$$\begin{bmatrix}0\\0\end{bmatrix} = \begin{bmatrix}r_r & 0\\ 0 & r_r\end{bmatrix}\cdot\begin{bmatrix}i^r_{dr}\\ i^r_{qr}\end{bmatrix} + \frac{d}{dt}\begin{bmatrix}\lambda^r_{dr}\\ \lambda^r_{qr}\end{bmatrix} \tag{25}$$

$$\begin{bmatrix}\lambda^r_{dr}\\ \lambda^r_{qr}\end{bmatrix} = \begin{bmatrix}\sqrt{M_d M_q} & 0\\ 0 & \sqrt{M_d M_q}\end{bmatrix}\cdot\begin{bmatrix}i^r_{ds}\\ i^r_{qs}\end{bmatrix} + \begin{bmatrix}L_r & 0\\ 0 & L_r\end{bmatrix}\cdot\begin{bmatrix}i^r_{dr}\\ i^r_{qr}\end{bmatrix}. \tag{26}$$

Upon solving the rotor current vector from (26) and inserting the result into (25), a current model rotor flux estimator equation can be obtained:

$$\frac{d}{dt}\begin{bmatrix}\lambda^r_{dr}\\ \lambda^r_{qr}\end{bmatrix} + \frac{r_r}{L_r}\begin{bmatrix}\lambda^r_{dr}\\ \lambda^r_{qr}\end{bmatrix} = \begin{bmatrix}\frac{r_r}{L_r}\sqrt{M_d M_q} & 0\\ 0 & \frac{r_r}{L_r}\sqrt{M_d M_q}\end{bmatrix}\cdot\begin{bmatrix}i^s_{ds}\\ i^s_{qs}\end{bmatrix}. \tag{27}$$

The advantage of this implementation is that it is linear and has real eigenvalues. Moreover, it requires relative rotor position rather than rotor velocity as is required by an implementation in the stationary reference frame [6]. The block diagrams of the direct field-oriented controller and the flux estimator are shown in Fig. 4 and Fig. 5.

III. SYSTEM IMPLEMENTATION AND EXPERIMENTAL RESULTS

A. Current Regulation Scheme Implementation and Experimental Results

The current regulation scheme illustrated in [1] has been

implemented in hardware as shown in Fig. 6. In Fig. 6, the current references and the machine EMF vector on d-q plane are provided by a DSP according to the machine torque control requirement. Machine phase currents are transformed to the d-q plane and the z_1-z_2 plane by a 4 by 4 transformation matrix that is derived from the stator decomposition transformation [1] subject to the constraint that the five phase machine windings are tied to a single neutral.

The positions of the current error vectors on both of the d-q and the z_1-z_2 planes as well as the position of vector E [1] are each represented by a three-digit binary number b2,b1,b0. Because a three-digit binary number is used as a position code, the d-q plane and the z_1-z_2 plane are divided into eight sections accordingly as shown in Fig. 7 a) and b), where only a portion of the d-q and the z_1-z_2 voltage vector planes [1] are drawn. The rules for the vector position coding are (take ΔI_{dq} as an example):

b2=0, if $|\Delta i_d|<|\Delta i_q|$; b2=1, if $|\Delta i_d|>|\Delta i_q|$;
b1=0, if $\Delta i_d<0$; b1=1, if $\Delta i_d>0$;
b0=0, if $\Delta i_q<0$; b0=1, if $\Delta i_q>0$.

The three three-digit codes are cascaded to form a nine-digit binary code and it provides 512 addresses to the EPROM in Fig. 6. A computer program was written to evaluate each of the 512 combinations to determine which switching mode should be stored in the EPROM for each case. For example, for the positions of the vectors shown in Fig. 7 a) and b), the address for the EPROM is 111 100 100. In this case, the derivative of the current error vector on d-q plane will be vector **A** if switching mode #6 is selected, or vector **B**, if #14 is selected. As can be seen from Fig. 7 a), both vector **A** and **B** can be used to decrease the current error ΔI_{dq} on the d-q plane. However, if mode #14 is selected, the current error on z_1-z_2 plane will be further increased. Therefore, the mode #6 should be selected and stored in the EPROM. The sampling frequency of the current regulator is controlled by the timing block in Fig. 6. It was set at 40 KHz, corresponding to a switching frequency about 10 KHz for each switch in the inverter.

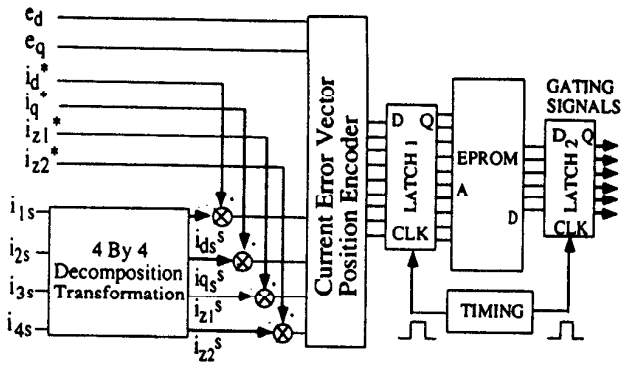

Fig. 6 Block Diagram of Current Regulator

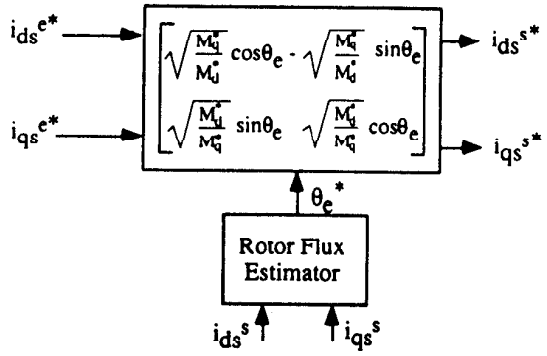

Fig. 4 Block Diagram of Direct Field-Oriented Control

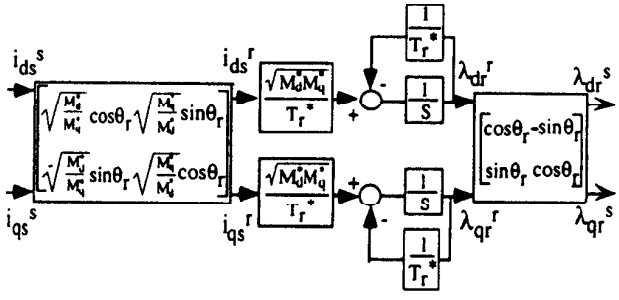

Fig. 5 Rotor Flux Estimator

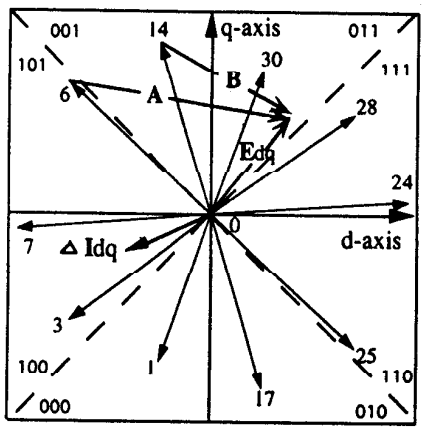

a)

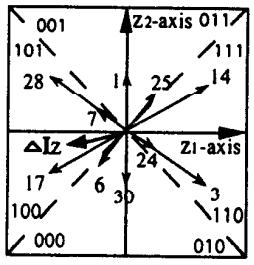

b)

Fig. 7.a) D-q Plane Inverter Voltage Vectors
b) Z_1-z_2 Plane Inverter Voltage Vectors

Fig. 8 shows the experimental results of the double-plane current regulator. The performance of the current regulator on the d-q plane is depicted in Fig. 8 a). To overcome the structure unbalance of the machine and obtain smooth output torque, the qs-axis and ds-axis current command amplitude ratio should be $\frac{M_d}{M_q}$, which can be determined from the stator current transformation (14). The results shown in Fig. 8 a) indicate that very good current regulation performance has been achieved on the d-q plane. Fig. 8. b) describes the

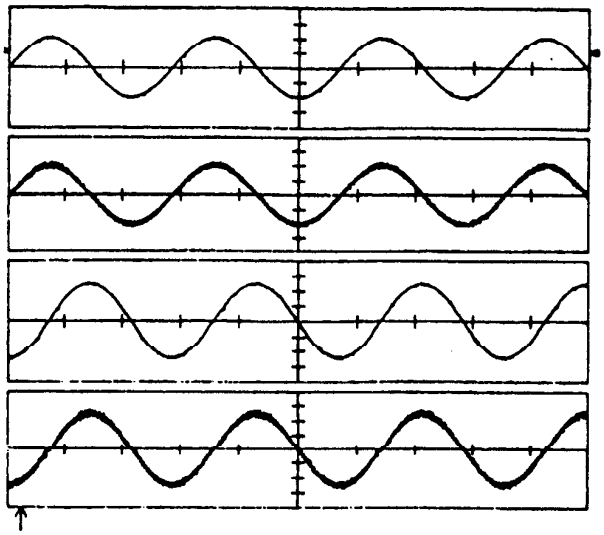

a)

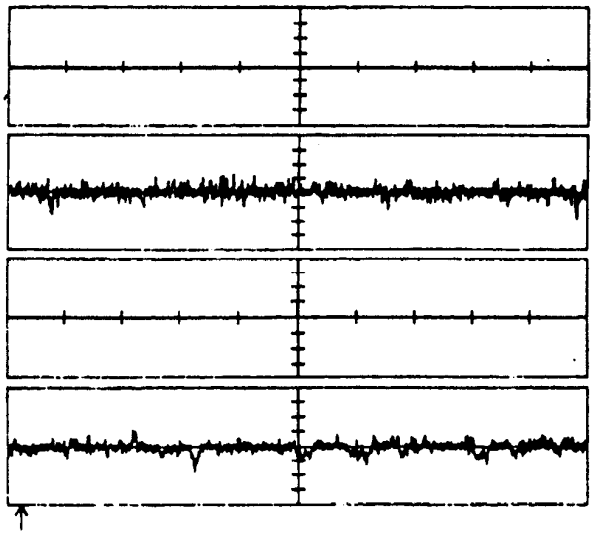

b)

Fig. 8 Experimental Results of Double-Plane Current Regulation
Time: 20 ms /div.;
a) Trace 1-4 (5 A/div.): d^s-axis current reference; d^s-axis current; q^s-axis current reference; q^s-axis current.
b) Trace 1-4 (5 A/div.): $z_1{}^s$-axis current reference; $z_1{}^s$-axis current; $z_2{}^s$-axis current reference; $z_2{}^s$-axis current.

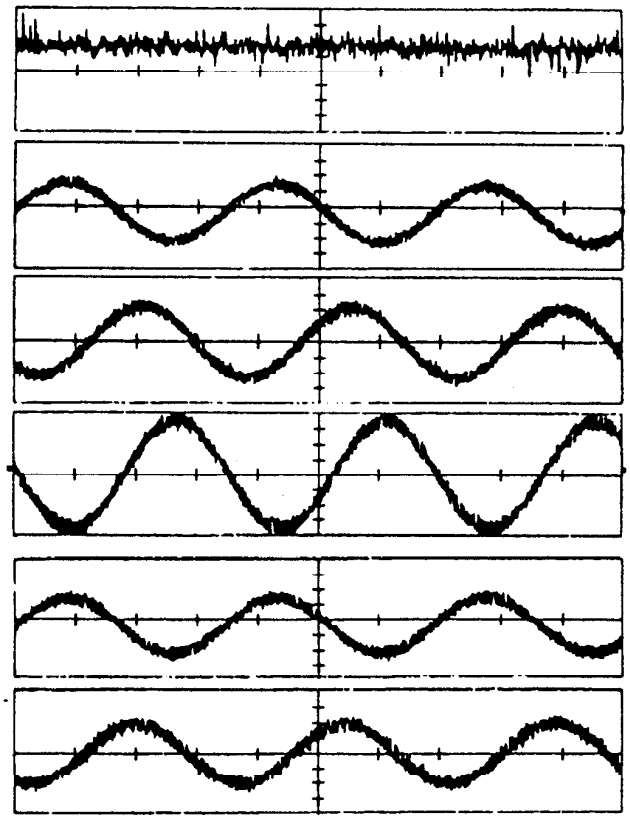

Fig. 9 Experimental Results: Machine Torque and Five Phase Currents
Time: 20 ms/div.;
Trace 1: machine torque (4 N.m/div.);
Trace 2-6: phase 1, 3, 5, 2, 4, currents (2 A/div.).

current regulation on the zero sequence plane. Since currents on this plane do not produce any torque, the current commands on this plane were set to be zero values to minimize the zero sequence current components and thus reduce the I^2R loss in the machine. The measured machine torque and the five phase real currents, which are regulated as a result of the double-plane current regulation, are shown in Fig. 9. As predicted analytically, smooth machine torque is obtained with the designed unbalanced stator excitation.

B. Experimental Verification of Field-Oriented Control

The entire drive system examined in this paper has been constructed to verify the developed analysis and control technique. The implementation uses IGBT's for the power switching devices and a MOTOROLA DSP56000 microprocessor for the controller. A five horsepower, four pole induction machine with thirty six stator slots was rewound to form a six pole, dual three phase machine for the test. The measured parameters of the machine are:

r_s=0.71 Ω
r_r=1.29 Ω

L_{ls}=4.41 mh
L_{lr}=4.41 mh
L_{ms}=16.3 mh.

The block diagram of the drive system is shown in Fig. 10 and the experimental results are shown in Fig. 11 and 12. The results in Fig. 11 describes the system response to step changes of torque command between 3.0 and 8.0 N-m. It can be observed that the machine torque responds very rapidly to the step changes in torque command and so does the stator current, both in its phase and amplitude. The rotor flux (shown in rotor reference frame) responses to the step changes of machine torque by changing its frequency (slip

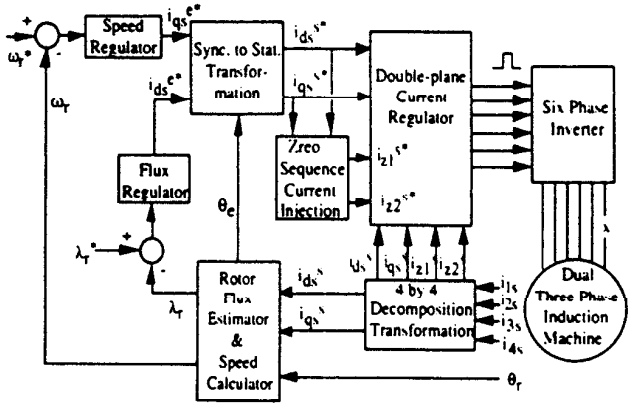

Fig. 10 Experimental System Block Diagram

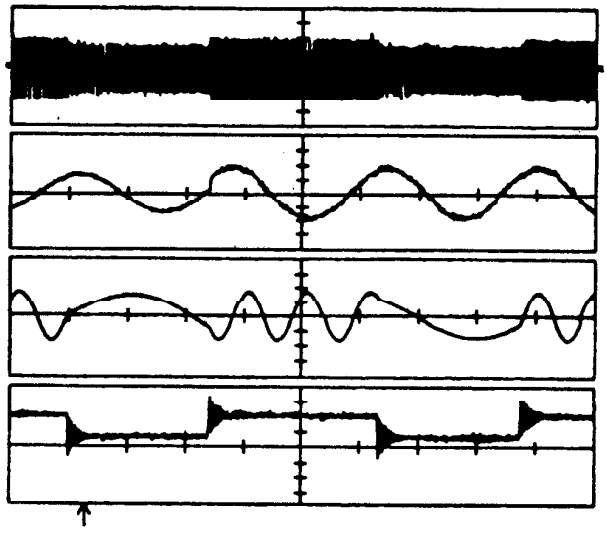

Fig. 11 Experimental Results: Demonstration of Field-Oriented Control
Time: 0.5 s/div.;
Trace 1: stator current (5 A/div.);
Trace 2: Stator current expanded in time axis (5 A/div.);
Trace 3: Estimated rotor flux linkage shown in rotor frame (0.1 Wb.Turn/div.);
Trace 4: Measured machine torque (4 N.m/div.).

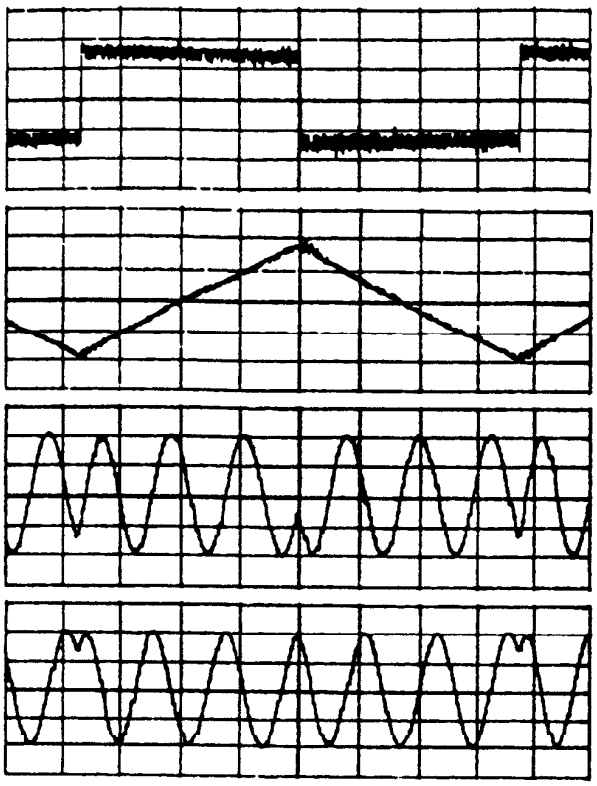

Fig. 12 Experimental Results: Demonstration of Field-Oriented Control
Time: 0.5 s/div.;
Trace 1: Calculated machine torque (5 N.m/div);
Trace 2: Measured rotor velocity (500 rpm./div);
Trace 3: Estimated d^r-axis rotor flux linkage (0.1 Wb.Turn/div);
Trace 4: Estimated q^r-axis rotor flux linkage (0.1 Wb.Turn/div).

frequency determined by (23)), while its amplitude is maintained constant. The high frequency oscillation found in the measured machine torque is the result of mechanical system resonance excited by the step change of the electromagnetic torque. Fig. 12 shows the experimental result when the system was tested by applying an alternating torque command between ± 8 N-m. In this case, the slip frequency remains constant since the torque command amplitude is constant. However, the sign of the slip frequency changes every time the torque changes its polarity, which can be observed from the leading position exchanges between the d^r-axis and q^r-axis rotor flux linkages. Fig. 12 also shows the speed of the machine. The triangular waveform of the speed (constant acceleration and deceleration in both directions) indicates that the machine torque is controlled very well.

C. Summary of Experimental Results

The experimental results have demonstrated that individual control of the torque producing components and the non-electromechanical energy conversion components of the machine variables are well managed by the double-plane

current regulator developed from the concept of decomposition. In particular, smooth machine torque has been achieved from the current control on the d-q plane. On the z_1-z_2 plane, the zero sequence components of stator current were minimized to reduce the I^2R loss.

The experimental results also presented very good agreement to the analyses of field-oriented control, which can be confirmed from the independent control of rotor flux linkage and electromagnetic torque. In summary, the analysis and control techniques developed in this paper have been verified.

IV CONCLUSIONS

Despite the existence of the zero sequence component defined in [1] and [2], a multi-phase induction machine is equivalent to a d-q winding two phase machine from the electromechanical energy conversion point of view. Torque control can be performed on the d-q plane using the field-oriented control technique developed for normal induction machines. However, for machines with an asymmetrical winding structure, unbalanced d-q plane stationary to synchronous reference frame transformation should be used to overcome the influence of the asymmetrical winding structure on torque producing (torque pulsating) and make the field-oriented control technique applicable. The transformation can be obtained by using stator MMF as an intermediate variable as described in this paper. With this transformation, the d-q model of the machine expressed in the synchronous reference frame is equivalent to a symmetrical machine model with its stator windings being the geometric mean of the d-q windings of the asymmetrical machine.

As far as the current regulation is concerned, zero sequence plane current regulation must be adopted together with the d-q plane current regulation for a multi-phase induction machine to reduce the zero sequence harmonic current.

V. REFERENCES

[1] Y. Zhao and T. A. Lipo, "Modeling and Field-Oriented Control of Multi-Phase Induction Machine With Structural Unbalance, Part I-Machine Modeling and Multi-Dimensional Current Regulation," companion paper.

[2] Y. Zhao and T. A. Lipo, "Space Vector PWM Control of Dual Three Phase Induction Machine Using Vector Space Decomposition," *IEEE Trans. on Ind. Appl.*, vol. 31, No. 5, Sept./Oct., 1995, pp. 1100-1109.

[3] T-H Liu, J-R Fu and T. A. Lipo, "A Strategy for Improving Reliability of Field-Oriented Controlled Induction Motor Drives," *IEEE Trans. on Ind. Appl.*, vol. 29, No. 5, Sept./Oct. 1993, pp. 910 918.

[4] T. A. Lipo and D. W. Novotny, *Dynamics and Control of AC Drives*, course notes for ECE711, University of Wisconsin-Madison, 1990.

[5] N. L. Schmitz, and D. W. Novotny, Introductory Electromechanics, Ronald Press, New York, 1965.

[6] P. L. Jansen, R. D. Lorenz "A Physically Insightful Approach to the Design and Accuracy Assessment of Flux Observers for Field Oriented Induction Machine Drives," *IEEE Trans. on Ind. Appl.*, vol. IA-30, No. 1, January/February, 1994, pp. 101-110.

[7] A. Nabae, S. Ogasawara, and H. Akagi, "A Novel Control Scheme for Current Controlled PWM Inverters," *IEEE Trans. on Ind. Appl.*, vol. IA-22, No. 4, July/August, 1981, pp. 697-701.

Yifan Zhao (S'91) received the B.S.E.E. degree from Jiaozuo College of Mining, China, in 1982, the M.S.E.E. degree from China University of Mining and Technology, in 1985, and the Ph.D. degree in electrical engineering from the University of Wisconsin-Madison, in 1995.

He was with the Industrial Automation Department, China University of Mining and Technology from 1985 to 1990 and worked as a university researcher. He is presently an Electrical Engineer at the Corporate Research and Development Center, General Electric Company. His research interests include microprocessor-based control systems, electrical machines and drives, and power electronics circuits.

Thomas A. Lipo (M'64-SM'71-F'87) is a native of Milwaukee Wisconsin. He received his B.E.E. and M.S.E.E. degrees from Marquette University, Milwaukee, WI in 1962 and 1964 and the Ph.D. degree in electrical engineering from the University of Wisconsin in 1968. From 1969 to 1979 he was an Electrical Engineer in the Power Electronics Laboratory of Corporate Research and Development of the General Electric Company, Schenectady NY. He became Professor of Electrical Engineering at Purdue University in 1979 and in 1981 he joined the University of Wisconsin in the same capacity where he is presently the W.W. Grainger Professor for Power Electronics and Electrical Machines.

In 1986 Dr. Lipo received the Outstanding Achievement Award from the IEEE Industry Applications Society for his contributions to the field of ac drives and in 1990 he received the William E. Newell Award of the IEEE Power Electronics Society for contributions to field of power electronics. He has recently received the 1995 Nicola Tesla IEEE Field Award "for pioneering contributions to simulation of and application to electric machinery in solid-state ac motor drives". Dr. Lipo has served in various capacities for three IEEE Societies including President of IAS in 1994.